mori et al., 2000) in fractions enriched in synaptic vesicles (LP2) (Fig. 2*B*). Pronase treatment led to the loss of the VGAT-N epitope (Fig. 2*C*). In contrast, probing of blots with anti-VGAT-C (AA 510–525) and anti-VGAT-lum1 (AA171–184) yielded distinct bands showing that the epitopes were protected against proteolysis within the SV lumen (Fig. 2*C*). Because pronase treatment degrades all regions exposed on the vesicle surface, our refined topology model (Fig. 1*B*) predicts peptide fragments of 10.4 kDa and 3.9 kDa for the anti-VGAT-lum1 and anti-VGAT-C, respectively. Indeed, anti-VGAT-lum1 detected a proteolytic fragment of the expected size. However, the major protected C-terminal fragment migrated as a ~12 kDa protein while only a weaker signal of the expected size was detectable. No signals were obtained after pronase treatment with antibodies directed against the C termini of VGLUT1, VGLUT2 and VAChT, in agreement with their predicted cytoplasmic localization.

To confirm that intravesicular epitopes remained protected during pronase treatment we monitored the cleavage of Syt1 using antibodies specific for the N-terminal intraluminal and C-terminal cytoplasmic domains, respectively. While the cytoplasmic epitope was lost, a fragment of the expected size was detected by the N-terminal antibody (Fig. 2*C*). Furthermore, trypsin treatment coupled with mass spectrometry of digested fragments revealed four additional cytosolic peptide fragments (supplemental Fig. 1, available at www.jneurosci.org as supplemental material). Three of these fragments covered the cytosolic N terminus while one corresponds to the third cytoplasmic loop (Fig. 1*B*; supplemental Fig. 1, available at www.jneurosci.org as supplemental material) thus lending further support to our refined model of VGAT topology.

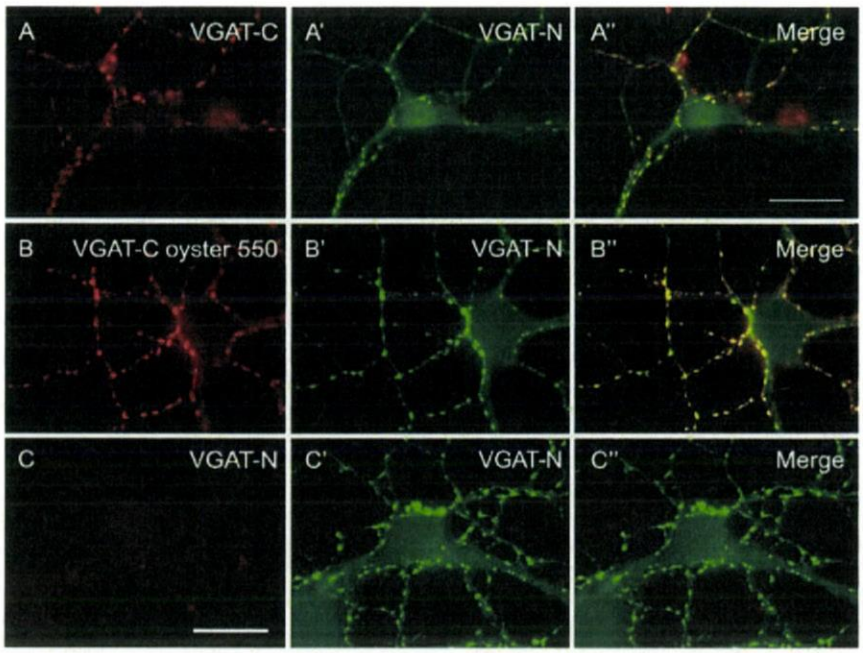

Figure 3. Labeling of live GABAergic neurons with anti-VGAT-C. ***A–A''***, Uptake of anti-VGAT-C at inhibitory terminals stimulated by 55 mM K^+. Incorporated antibodies were visualized after fixation and permeabilization by indirect immunofluorescence. Note prominent colocalization with anti-VGAT-N. ***B–B''***, Detection of inhibitory axon terminals through uptake of Oyster550-anti-VGAT-C of live rat hippocampal neurons *in vitro*. Anti-VGAT-N was applied indirectly on fixed cells. ***C–C''***, Control showing the lack of anti-VGAT-N uptake (cytoplasmic epitope) by cultured hippocampal neurons; subsequent counterstaining with monoclonal anti-VGAT-N. Yellow/orange color denotes colocalization. Scale bar, 20 μm.

Histochemical localization of VGAT C terminus

Immunoperoxidase (Fig. 2*D–G*) and immunofluorescence (supplemental Fig. 2, available at www.jneurosci.org as supplemental material) histochemistry of free-floating vibratome sections processed with or without detergent was performed to confirm the native folding of the two termini of VGAT across SV membranes. Since synapses at the tissue surface are cut open by the vibratome blade antibodies can directly access the surface of SVs (Chaudhry et al., 1998). In the absence of a detergent, anti-VGAT-N reveals punctate terminal-like staining concentrated e.g., in the hippocampal pyramidal cell layer (Fig. 2*D*) given its free access to the cytosolic VGAT N terminus (Boulland et al., 2008). In contrast, anti-VGAT-C failed to reveal any punctate staining even at high concentrations that otherwise lead to unspecific nuclear staining (Fig. 2*E*). Terminal-like labeling with anti-VGAT-C when its penetration is facilitated by Triton X-100 bolsters a luminal localization of this epitope (Fig. 2*F, G*). Immunofluorescence labeling and laser-scanning microscopy yielded identical results (supplemental Fig. 2, available at www.jneurosci.org as supplemental material). Overall, these data demonstrate that the C terminus of VGAT is localized in the lumen of SVs.

Dynamic labeling of GABAergic synapses *in vitro*

During recycling of SVs, luminal epitopes of SV proteins are temporarily exposed at the cell surface. Proteins recognizing these epitopes can bind to the surface of intact neurons and may become internalized by endocytosis. Indeed, antibodies directed against the N-terminal domain of Syt1 are widely used to selectively label recycling vesicles in nerve terminals (Kraszewski et al., 1995). Therefore, we tested whether anti-VGAT-C can be used to selectively label GABA release sites.

Immunohistochemistry on perfusion-fixed brain sections showed that both unlabeled and Oyster550-labeled anti-VGAT-C selectively recognize GABAergic axon terminals (supplemental Fig. 3, available at www.jneurosci.org as supplemental material). Next, we incubated live neurons for 5 min with anti-VGAT-C (5 μg/ml) with or without Oyster550 label at 37°C. Upon K^+-induced depolarization, bright immunofluorescence reminiscent of synaptic puncta were observed (Fig. 3*A, B*). Selective targeting of unlabeled anti-VGAT-C-derived (Fig. 3*A*) or Oyster550-anti-VGAT-C (Fig. 3*B*) to GABAergic synapses was verified by colocalization with anti-VGAT-N. Negligible or no labeling of inhibitory terminals was obtained by applying either cytoplasmic anti-VGAT-N (Fig. 3*C*) or anti-VGAT-lum1 (data not shown). Application of a CypHer5E-anti-VGAT-C conjugate that only produces fluorescence signal in endocytic vesicles at acidic pH also revealed terminal labeling (supplemental Fig. 4, available at www.jneurosci.org as supplemental material). These data reinforce the luminal localization of VGAT C terminus and its accessibility to antibodies in active synapses.

To verify that Oyster550-anti-VGAT-C is selectively taken up by GABAergic synapses, antibody- and mock-treated autaptic cultures

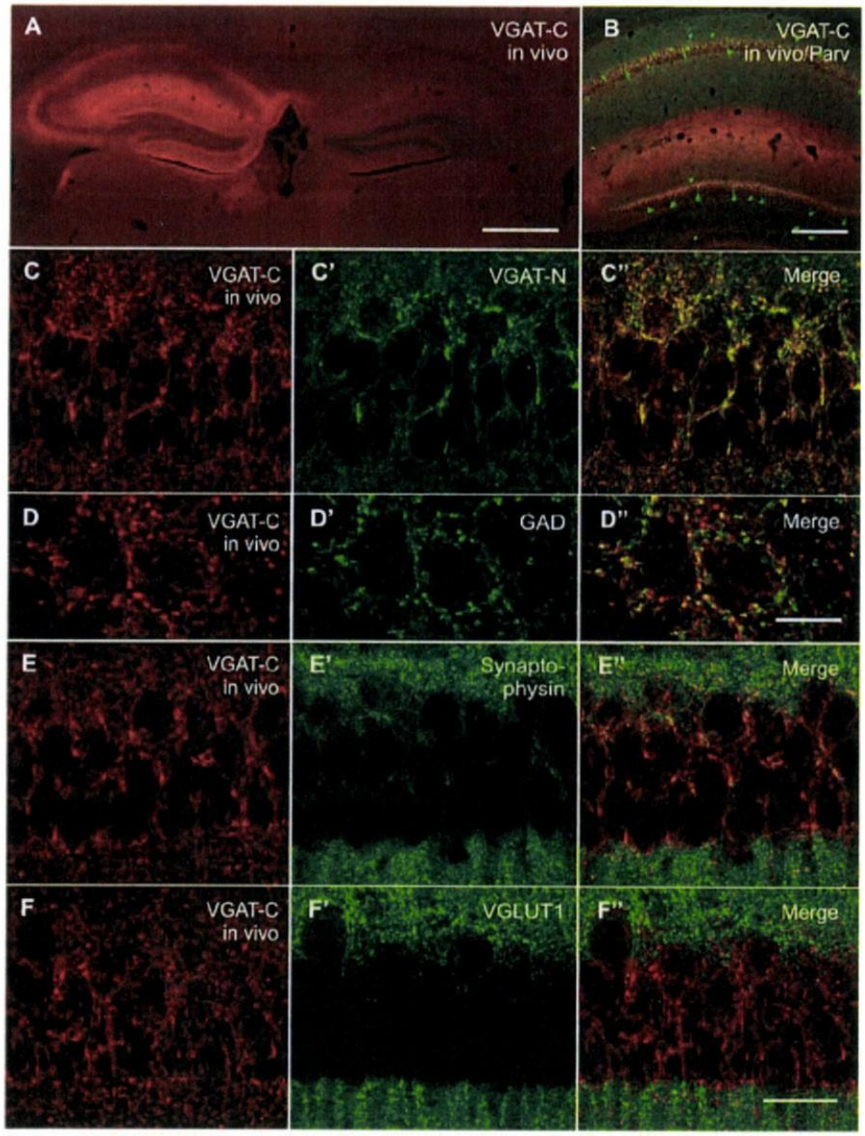

Figure 4. *In vivo* labeling of GABAergic synapses in mouse hippocampus. Direct *in vivo* VGAT-C labeling in the CA1 region and dentate gyrus (DG) 48 h after intrahippocampal antibody infusion combined with indirect Cy2-immunostaining of parvalbumin, VGAT-N, GAD, synaptophysin, and VGLUT1. ***A***, Distribution of Oyster550-anti-VGAT-C in the injected (left) hippocampal hemisphere. ***B***, Cy3-anti-VGAT-C in the injected hippocampal hemisphere counterstained with antibodies against parvalbumin. ***C–C''***, Oyster550-anti-VGAT-C counterstained with anti-VGAT-N in the CA1 region and combined with anti-GAD in DG (***D–D''***). Partial coexpression of Oyster550-anti-VGAT-C and synaptophysin in select GABAergic synapses (***E–E''***). Lack of coexistence of Oyster550-anti-VGAT-C and VGLUT1 in the CA1 region (***F–F''***). Scale bars: 1 mm (***A***), 250 μm (***B***), 10 μm (***D***), 30 μm (***F***, also valid for ***C***, ***E***).

of striatal and hippocampal neurons were analyzed by whole cell recordings in voltage clamp mode. Evoked synaptic responses recorded from labeled striatal neurons were exclusively of IPSC type whereas hippocampal neurons staying unlabeled after antibody treatment always exhibited EPSCs. Miniature IPSC amplitudes, their frequency and the readily releasable pool remained unchanged in Oyster550 anti-VGAT-C labeled cells, whereas the evoked IPSC charge was reduced by 46% relative to unlabeled neurons (supplemental Fig. 5, available at www.jneurosci.org as supplemental material). Anti-VGAT-C treated neurons showed a slight, but nonsignificant reduction in vesicular release probability.

In vivo labeling of GABAergic synapses

Our above experiments suggest that anti-VGAT-C may be a versatile tool to visualize GABAergic terminals also *in vivo*. Therefore, Oyster550-anti-VGAT-C was stereotaxically injected into the CA1 subfield of the hippocampus of adult mice. Bright red immunolabeling reminiscent of the laminar distribution of GABAergic synapses was evident in the injected hemisphere 48 h later (Fig. 4*A*,*B*), with labeled structures exhibiting coincident immunoreactivities for VGAT-N (Fig. 4*C*), GAD (Fig. 4*D*) and synaptophysin (Fig. 4*E*). High-resolution images revealed anti-VGAT-C immunoreactivity surrounding (rather than overlapping) GAD-immunopositive structures (Fig. 4*D*). *In vivo* labeling and VGLUT1 immunostaining produced distribution patterns complementary with that of indirect VGLUT1 localization (Fig. 4*F*) underscoring the specificity of anti-VGAT-C immunoreactivity. We conclude that fluorochromated antibodies specific for the C-terminal of VGAT can also be used to label GABAergic terminals in live animals.

Discussion

Here, we show that the C terminus of VGAT localizes to the SV lumen resulting in an uneven number of transmembrane domains. We also demonstrate that antibodies directed against this domain recognize VGAT in intact neurons and are sequestered by endocytosis without major long-term perturbation of synaptic functions, making these immunoreagents versatile tools to identify release sites of GABA and glycine and to study the kinetics of SV recycling in active synapses.

Our knowledge about the topology of VNTs is largely based on computer predictions that often lack experimental confirmation. The TMHMM algorithm predicted a VGAT transmembrane topology which shows major differences compared with previous models (McIntire et al., 1997). In contrast to the model proposed by McIntire et al. (1997), which agrees with most algorithms predicting transmembrane topologies, the AA 243–263 region is classified by the TMHMM algorithm as part of the first cytoplasmic loop rather than a transmembrane domain. Consequently, VGAT exhibits an uneven number of transmembrane domains whose orientation downstream from serine 242 is inversed with the C-terminal 14–16 residues being localized intraluminally instead of being exposed on the outer SV surface. Accordingly, the N and C-terminal and first luminal domains recognized by anti-VGAT-N, anti-VGAT-C and anti-VGAT-lum1, respectively, were differentially sensitive to pronase treatment of isolated SVs. Our proteolytic assays and mass spectrometry do not provide conclusive support for the exact membrane topology of VGAT. Nevertheless, these results unequivocally confirm that the entire N terminus and the loop containing AA 408–415 face the cytoplasm while both epitopes recognized by anti-VGAT-C and anti-VGAT-lum1 are localized in the lumen of SVs.

The major pronase-resistant C-terminal VGAT fragment migrated as ~10–15 kDa protein. This does not correspond to the expected ~3–4 kDa size of the fragment comprising the luminal C terminus and the last transmembrane domain which was only visible as a weaker signal. Apparently, the small size of the last putative cytoplasmic loop (5–14 AA, depending on the prediction algorithm) renders it partially resistant to proteolytic cleavage, as also reported for synaptogyrin (Stenius et al., 1995). The larger fragment probably represents the C terminus together with the preceding cytoplasmic and luminal loops and 3 transmembrane domains with a cumulative molecular weight of 10–11 kDa. In contrast, the C termini of VGLUT1, VGLUT2 and VAChT were completely degraded confirming the cytoplasmic localization of these protein epitopes. Thus, VGAT exhibits an exceptional transmembrane topology compared with other known VNTs.

VGAT is the only member of the SLC32 family with no other close mammalian relatives identified so far. Our observations underline the evolutionary distance between VGAT and other known VNTs, which belong to the SLC17 (VGLUT 1–3) or the SLC18 family (VMAT1, 2 and VAChT) (Gasnier, 2004). These latter transporter families are homologous to bacterial toxin/drug extruders (Chaudhry et al., 2008b) while VGAT is not. VGAT even shows significant structural differences when compared with other functionally related membrane located GABA transporters (GAT-1, 2, 3 and BGT-1; (Alexander et al., 2007). The refined VGAT topology with an uneven number of transmembrane domains suggests a closer relationship between VGAT and amino acid permeases in plants which share sequence homology (Wipf et al., 2002) and a similar transmembrane topology with a cytoplasmic localization of the N terminus and a C terminus residing on the outer surface of the plasmalemma (Chang and Bush, 1997). The transmembrane topology for VGAT may also implicate differences in its functional regulation compared with other VNTs whose cytosolic C termini are accessible for other regulatory proteins potentially modulating their function; e.g., endophilin regulation of VGLUT1 recycling (Voglmaier et al., 2006).

Short and transient exposure of live neurons to anti-VGAT-C is sufficient for antibody binding and internalization. Labeling is highly selective for GABAergic neurons indicating that anti-VGAT-C endocytosis is mediated by specific epitope binding and not by unspecific fluid phase uptake. Fluorochromated anti-VGAT-C exhibited a remarkable penetration *in vivo*. In a subset of synapses, anti-VGAT-C labeling closely surrounded, though did not entirely overlap, GAD immunoreactivity. This may be due to a sterical competition of internalized and perfusion-fixed anti-VGAT-C and subsequently applied anti-GAD. Interestingly, antibody uptake led to a 46% reduction of the overall evoked IPSC amplitude and slightly but not significantly reduced SV release probability. The individual miniature fusion events, their frequency and the readily releasable vesicle pool remained unchanged indicating that the presence of luminal anti-VGAT-C can lead to subsequent reduction of the efficiency of SV release but does not affect the translocation of GABA into SVs.

Understanding the precise spatial localization of the VGAT C terminus to the SV lumen is vital for exploiting the potential of our approach to live cell imaging and physiology models of inhibitory neurotransmission. Our confocal imaging studies present the possibility of using VGAT as a novel biomarker in studies aimed at elucidating organizing principles of inhibitory synapses. Combined use of *in vivo* labeling and tracer ligands holds promise for revealing novel synaptic circuitries and refined innervation patterns in the brain. Moreover, *in vivo* labeling of functionally intact and electrophysiologically active GABAergic terminals will yield a new dimension of understanding key features of inhibitory neurotransmission, and their perturbations in neuropathological conditions.

References

Alexander SP, Mathie A, Peters JA (2007) Guide to receptors and channels (GRAC), 2nd edition (2007 Revision). Br J Pharmacol 150:S1–S168.

Boulland J L, Jenstad M, Boekel AJ, Wouterlood FG, Edwards RH, Storm-Mathisen J, Chaudhry FA (2008) Vesicular glutamate and GABA transporters sort to distinct sets of vesicles in a population of presynaptic terminals. Cereb Cortex. Advance online publication. Retrieved May 22, 2008. doi:10.1093/cercor/bhn077

Chang HC, Bush DR (1997) Topology of NAT2, a prototypical example of a new family of amino acid transporters. J Biol Chem 272:30552–30557.

Chaudhry FA, Reimer RJ, Bellocchio EE, Danbolt NC, Osen KK, Edwards RH, Storm-Mathisen J (1998) The vesicular GABA transporter, VGAT, localizes to synaptic vesicles in sets of glycinergic as well as GABAergic neurons. J Neurosci 18:9733–9750.

Chaudhry FA, Boulland JL, Jenstad M, Bredahl MK, Edwards RH (2008a) Pharmacology of neurotransmitter transport into secretory vesicles. Handb Exp Pharmacol 184:77–106.

Chaudhry FA, Edwards RH, Fonnum F (2008b) Vesicular neurotransmitter transporters as targets for endogenous and exogenous toxic substances. Annu Rev Pharmacol Toxicol 48:277–301.

Erickson JD, Weihe E, Schäfer MK, Neale E, Williamson L, Bonner TI, Tao-Cheng JH, Eiden LE (1996a) The VAChT/ChAT "cholinergic gene locus": new aspects of genetic and vesicular regulation of cholinergic function. Prog Brain Res 109:69–82.

Erickson JD, Schafer MK, Bonner TI, Eiden LE, Weihe E (1996b) Distinct pharmacological properties and distribution in neurons and endocrine cells of two isoforms of the human vesicular monoamine transporter. Proc Natl Acad Sci U S A 93:5166–5171.

Gasnier B (2000) The loading of neurotransmitters into synaptic vesicles. Biochimie 82:327–337.

Gasnier B (2004) The SLC32 transporter, a key protein for the synaptic release of inhibitory amino acids. Pflugers Arch 447:756–759.

Gauthier-Campbell C, Bredt DS, Murphy TH, El-Husseini Ael-D (2004) Regulation of dendritic branching and filopodia formation in hippocampal neurons by specific acylated protein motifs. Mol Biol Cell 15:2205–2217.

Härtig W, Seeger J, Naumann T, Brauer K, Brückner G (1998) Selective in vivo fluorescence labelling of cholinergic neurons containing $p75^{NTR}$ in the rat basal forebrain. Brain Res 808:155–165.

Jahn R (1999) Recycling of synaptic vesicle membrane within nerve terminals. Brain Res Bull 50:313–314.

Klingauf J, Kavalali ET, Tsien RW (1998) Kinetics and regulation of fast endocytosis at hippocampal synapses. Nature 394:581–585.

Kraszewski K, Mundigl O, Daniell L, Verderio C, Matteoli M, De Camilli P (1995) Synaptic vesicle dynamics in living cultured hippocampal neurons visualized with CY3-conjugated antibodies directed against the lumenal domain of synaptotagmin. J Neurosci 15:4328–4342.

Laemmli UK (1970) Cleavage of structural proteins during the assembly of the head of bacteriophage T4. Nature 227:680–685.

Liu Y, Edwards RH (1997) The role of vesicular transport proteins in synaptic transmission and neural degeneration. Annu Rev Neurosci 20:125–156.

Masson J, Sagné C, Hamon M, El Mestikawy S (1999) Neurotransmitter transporters in the central nervous system. Pharmacol Rev 51:439–464.

McIntire SL, Reimer RJ, Schuske K, Edwards RH, Jorgensen EM (1997) Identification and characterization of the vesicular GABA transporter. Nature 389:870–876.

Nagy A, Baker RR, Morris SJ, Whittaker VP (1976) The preparation and characterization of synaptic vesicles of high purity. Brain Res 109:285–309.

Perin MS, Brose N, Jahn R, Südhof TC (1991) Domain structure of synaptotagmin (p65). J Biol Chem 266:623–629.

Pyott SJ, Rosenmund C (2002) The effects of temperature on vesicular supply and release in autaptic cultures of rat and mouse hippocampal neurons. J Physiol 593:523–535.

Schägger H, von Jagow G (1987) Tricine-sodium dodecyl sulfate-polyacrylamide gel electrophoresis for the separation of proteins in the range from 1 to 100 kDa. Anal Biochem 166:368–379.

Schneider WJ, Slaughter CJ, Goldstein JL, Anderson RG, Capra JD, Brown MS (1983) Use of antipeptide antibodies to demonstrate external orientation of the NH2-terminus of the low density lipoprotein receptor in the plasma membrane of fibroblasts. J Cell Biol 97:1635–1640.

Schoch S, Gundelfinger ED (2006) Molecular organization of the presynaptic active zone. Cell Tissue Res 326:379–391.

Siegemund T, Paulke BR, Schmiedel H, Bordag N, Hoffmann A, Harkany T, Tanila H, Kacza J, Härtig W (2006) Thioflavins released from nanoparticles target fibrillar amyloid beta in the hippocampus of APP/PS1 transgenic mice. Int J Dev Neurosci 24:195–201.

Stenius K, Janz R, Südhof TC, Jahn R (1995) Structure of synaptogyrin (p29) defines novel synaptic vesicle protein. J Cell Biol 131:1801–1809.

Sudhof TC (2004) The synaptic vesicle cycle. Annu Rev Neurosci 27:509–547.

Takamori S (2006) VGLUTs: 'exciting' times for glutamatergic research? Neurosci Res 55:343–351.

Takamori S, Riedel D, Jahn R (2000) Immunoisolation of GABA-specific synaptic vesicles defines a functionally distinct subset of synaptic vesicles. J Neurosci 20:4904–4911.

Towbin H, Staehelin T, Gordon J (1979) Electrophoretic transfer of proteins from polyacrylamide gels to nitrocellulose sheets: procedure and some applications. Proc Natl Acad Sci U S A 76:4350–4354.

Voglmaier SM, Kam K, Yang H, Fortin DL, Hua Z, Nicoll RA, Edwards RH (2006) Distinct endocytic pathways control the rate and extent of synaptic vesicle protein recycling. Neuron 51:71–84.

Wipf D, Ludewig U, Tegeder M, Rentsch D, Koch W, Frommer WB (2002) Conservation of amino acid transporters in fungi, plants and animals. Trends Biochem Sci 27:139–147.